

# Survivability of a star cluster in a dispersing molecular cloud

Hui-Chen Chen<sup>1</sup> \* and Chung-Ming Ko<sup>1,2\*</sup>

<sup>1</sup> *Institute of Astronomy, National Central University, Taiwan*

<sup>2</sup> *Department of Physics and Center for Complex Systems, National Central University, Taiwan*

Accepted . Received ; in original form 2008 April ?

## ABSTRACT

Star clusters are formed in molecular clouds which are believed to be the birth places of most stars. From recent observational data, Lada & Lada (2003) estimated that only 4% to 7% of the clusters embedded inside molecular clouds have survived. An important mechanism for the disruption of embedded (bound)-clusters is the dispersion of the parent cloud by UV radiation, stellar winds and/or supernova explosions. In this work we study the effect of this mechanism by N-body simulations. We find that most embedded-clusters survive for more than 30 Myr even when different initial conditions of the cluster may introduce some minor variations, but the general result is rather robust.

**Key words:** stellar dynamics - methods: N-body simulations - galaxies: star clusters.

## 1 INTRODUCTION

Stellar clusters are among the most interesting objects in astronomy. We are interested in how they form, how they evolve and how they die. Observations gave the evidence that most stars are not born independently but in stellar clusters or stellar associations which are formed in molecular clouds (e.g., Lada & Lada (2003)). Due to the limits of observational techniques, we do not know in detail the relation between the clusters and the parent molecular clouds. It is believed that stars are born in clusters and become field stars after the clusters disassociate.

Recently, near infrared observational data (2MASS, Two Micron All Sky Survey project at IPAC/Caltech) have shown that the number of embedded clusters is much higher than the number of optical clusters for which the parent clouds have already dissipated and that the survival probability for embedded clusters in Milky Way is about 4% to 7% (Lada & Lada (2003)). Similar evidences for infant mortality are found in Antennae galaxies (Fall et al. (2005)), Small Magellanic Cloud (Chandar et al. (2006)) and NGC1313 (Pellerin et al. (2007)).

These imply that clusters are likely to be disrupted before the clouds are dissipated completely. Since the time the clusters were born, they are under constant threats from their surrounding environment.

Galactic tidal forces, close encounters with giant molecular clouds (see, e.g., Gieles et al. (2006)), shock heat-

ing and mass loss by massive member stars (see e.g., Boily & Kroupa (2003a,b)) are possible disruption mechanisms. Nonetheless, most of these mechanisms have a destruction timescale longer than the upper limit of the lifetime of molecular clouds which is about few to few tens Myr (see e.g., Blitz & Shu (1980), Elmegreen (2000), Hartmann et al. (2001), Bonnell et al. (2006)). The results of CO observations in the Galaxy suggest that the lifetime of molecular clouds is of the order of 10 Myr (see, e.g., Leisawitz et al. (1989)). The estimation of the timescale for photoevaporation and statistics on the expected numbers of stars per cloud show that giant molecular clouds of mass  $10^6 M_{\odot}$  are expected to survive for about 30 Myr (see, e.g., Williams & McKee (1997)).

Generally speaking, mechanisms with destruction timescales less than the lifetime of the clouds should be responsible for the low survival probability mentioned above. In this work, we focus on the role played by the dispersion of the parent cloud on the early evolution of the embedded clusters.

In the beginning, the clusters are bound to their parent molecular cloud. As the cloud dissipates, the binding energy from the cloud decreases and the stellar systems become out of equilibrium. Once out of equilibrium, they may expand or dissociate completely.

The survivability of clusters under gas dispersion has been examined in the past and extensive N-body simulations were performed in the past few years (see e.g. Lada et al. (1984), Goodwin (1997), Boily & Kroupa (2003b), Baumgardt & Kroupa (2007), Bastian & Goodwin (2006), Goodwin & Bastian (2006)). In a large set of sim-

\* E-mail: huichen@astro.ncu.edu.tw (HCC); cmko@astro.ncu.edu.tw (CMK)

ulations, Baumgardt & Kroupa (2007) studied the dispersal of the residual gas by decreasing the mass with different star formation efficiency (SFE), and in different tidal fields. They concluded that the clusters had to form with  $\text{SFE} \geq 30\%$  in order to survive gas expulsion, and the external tidal fields have significant influences only if the ratio of half mass radius to tidal radius is larger than 0.05. Goodwin & Bastian (2006) and Bastian & Goodwin (2006) addressed similar problem and found that the embedded clusters would be destroyed within a few tens of Myr if the “effective star formation efficiency”  $\leq 30\%$  ( $\text{eSFE} = 1/2Q$ , and  $Q=0.5$  for virial equilibrium).

The paper is organized as follows. In Section 2, we describe the model and parameters for our simulations. In Section 3, we present and discuss the results and statistics of the simulations. A summary and some remarks are provided in Section 4.

## 2 MODEL AND SIMULATION

We intend to learn the behaviour of a star cluster in a dispersing molecular cloud. For simplicity, we do not consider the feedback of the cluster onto the cloud, and the cloud is simply represented by its gravitational force. In other words, we study the behaviour of a star cluster in a time varying gravitational field. We adopted the N-body simulation code NBODY2 developed by Aarseth (2001) for our calculations. As a first attempt, we assume a spherically symmetric external potential (representing the molecular cloud), and initially the centre of mass of the cluster coincides with the centre of the potential. The initial spatial and velocity distributions of the cluster depend on the initial profile of the external potential (i.e., the initial mass and compactness of the cloud). Subsequent evolution of the cluster depends, of course, on its initial distribution and the rate of dispersion of the external potential.

### 2.1 Model for the cloud

The cloud is represented by a Plummer potential,

$$\Phi_P = \frac{-GM_b}{\sqrt{r^2 + a^2}}, \quad (1)$$

where  $M_b$  is the total mass of the cloud,  $a$  is the length scale of the potential and  $G$  is the gravitational constant. To model the dispersion of the cloud we consider the potential to evolve in time according to

$$a = a_0 e^{\alpha t}, \quad (2)$$

where  $a_0$  and  $\alpha$  are the initial length scale and the dispersion rate of the cloud, respectively. The total mass of the cloud remains constant as the length scale increases with time. Stellar masses would change by stellar evolution. However, since we run our simulations for 30 Myr only (which is about the maximum life time of molecular clouds) and massive stars are rare, hence we do not consider stellar evolution in this work.

There are three parameters for the cloud: (i) dispersion rate  $\alpha$ , (ii) total mass  $M_b$ , and (iii) initial length scale  $a_0$ .

**Table 1.** Dispersion rates of the cloud

index	A	B	C	D	E
$\alpha$	0.1	0.2	0.3	0.4	0.5
$t_e$ [Myr]	3.3	1.5	1.1	0.75	0.625

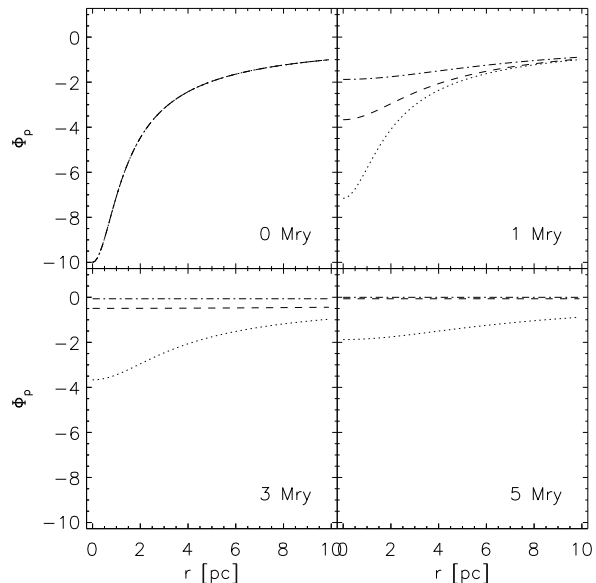


**Figure 1.** Evolution of the cloud potential in dispersion rate of  $\alpha=0.1$  (dotted line), 0.3 (dashed line) and 0.5 (dash-dotted line), whose e-fold times are  $t_e=3.3$ , 1.1 and 0.625 Myr, respectively. At 0 Myr, the potentials are the same. After 1 Myr, every one becomes shallower in difference degree. At 3 Myr, the two cases with  $t_e=1.1$  and 0.625 Myr approach zero. At 5 Myr, even the case with  $t_e=3.3$  Myr becomes rather flat.

#### 2.1.1 Dispersion rate $\alpha$

We take  $\alpha$  as 0.1, 0.2, 0.3, 0.4, 0.5 in the unit used by the code. These correspond to a e-fold time  $t_e$  as 3.3, 1.5, 1.1, 0.75, 0.625 Myr in real unit (see Table 1).

Fig. 1 shows how the cloud potential evolves. The potentials of  $\alpha = 0.3$  and 0.5 are almost zero after 5 Myr. Even for  $\alpha = 0.1$ , the potential is rather flat after 5 Myr. We would expect the cloud exerts no effect on the cluster after a relatively short time in these dispersion rates. The seed of destruction is planted (if at all) only in the early dispersion stage of the cloud.

#### 2.1.2 Total mass $M_b$

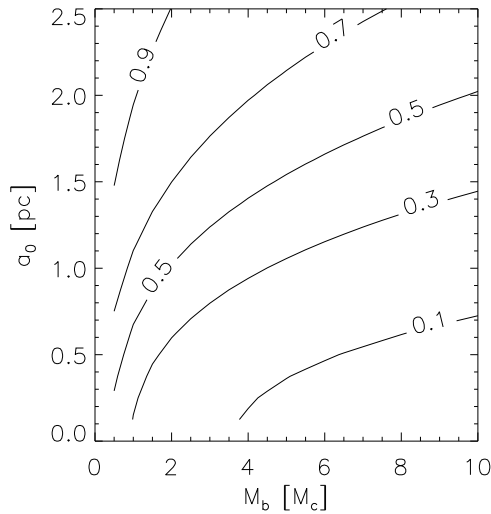
The more massive the cloud is the more influence on the cluster is. We consider the total mass of the cloud  $M_b$  from 0.5 to 10 cluster mass  $M_c$  as listed in Table 2. We note that  $M_c = 2500M_\odot$  in all our simulations. Generally, the star formation efficiency is defined as

$$\eta = \frac{M_c}{M_c + M_b}. \quad (3)$$

The mass range we choose corresponds to  $\eta = 50$  to 9%.

**Table 2.** Total cloud mass in unit of cluster mass

index	01	02	03	04	05	06	07
$M_b [M_c]$	0.5	1	1.5	2	2.5	3	3.5
	08	09	10	11	12	13	14
$M_b [M_c]$	4	4.5	5	5.5	6	6.5	7
	15	16	17	18	19	20	
$M_b [M_c]$	7.5	8	8.5	9	9.5	10	

**Figure 2.** Contour of  $\beta$ , the cluster-cloud mass ratio at  $r_{40}$  of the clusters. Cloud and cluster have the same mass within  $r_{40}$  when  $\beta = 0.5$ .

For later discussions, we introduce the cluster-cloud mass ratio at 40% Lagrangian radius of the cluster

$$\beta = \frac{M_{c,r40}}{M_{c,r40} + M_{b,r40}}, \quad (4)$$

where  $M_{b,r40}$  is the mass of the cloud within the initial 40% Lagrangian radius of the cluster.  $M_{b,r40}$  depends on  $a_0$  and  $M_b$ . Fig. 2 shows the contour of  $\beta$  in the parameter space ( $M_b, a_0$ ). Note that  $M_{c,r40}$  is constant (in fact  $1000M_\odot$ ) in our simulations (as  $M_c = 2500M_\odot$  in all our simulations).

From its definition,  $\beta$  describes star formation efficiency in a certain sense. In fact, there is an explicit relation between  $\beta$  and  $\eta$  (the commonly defined star formation efficiency),

$$\frac{1}{\beta} = 1 + \frac{r_{40}^3}{M_{c,r40}(r_{40}^2 + a^2)^{3/2}} \left( \frac{1}{\eta - 1} \right). \quad (5)$$

We find that our simulation results on the effect of the parent cloud on the cluster is better described by  $\beta$ . Further discussion will be given later and the 40% Lagrangian radius of cluster will be denoted as  $r_{40}$  hereafter.

### 2.1.3 Initial length scale $a_0$

The length scale of the Plummer potential describes the compactness of the cloud. The more compact the cloud is the more its effect on the cluster is when it disperses. We

**Table 3.** Initial length scale of the cloud

index	a	b	c	d	e	f	g
$a_0$ [pc]	0.125	0.25	0.375	0.5	0.625	0.75	0.875
	h	i	j	k	l	m	n
$a_0$ [pc]	1	1.125	1.25	1.375	1.5	1.625	1.75
	o	p	q	r	s	t	
$a_0$ [pc]	1.875	2	2.125	2.25	2.375	2.5	

consider  $a_0$  from 0.125 pc (compact) to 2.5 pc (loose) as listed in Table 3.

Each set ( $\alpha, M_b, a_0$ ) represents a model, and we name the model by the indices in Tables 1, 2 & 3. For example, B10h corresponds to dispersion rate  $\alpha = 0.2$  (i.e.,  $t_e = 1.5$  Myr), total cloud mass  $M_b = 5M_c = 12500M_\odot$ , and initial length scale of cloud  $a_0 = 1$  pc.

## 2.2 Model for the cluster

### 2.2.1 Initial conditions

The star cluster is prepared according to a Plummer distribution both in physical positions and velocities, which are required to achieve virial equilibrium. Note that the fact the cluster is in virial equilibrium does not mean that it is also in dynamical equilibrium (see e.g., Lada et al. (1984), Goodwin (1997)). In fact, right after we start the simulation, the cluster oscillates (shrinking and expanding) for a few times before settle down to a smoother (and more “natural”) distribution (see Fig. 3). We, therefore, generate initial conditions according to the following steps:

- generate a cluster with a Plummer distribution and a size about 1 pc; and we called this initial condition IC-0;
- put the cluster into a molecular cloud, represented as a Plummer potential, with its centre of mass coincides with the centre of the potential;
- turn off the cloud dispersion (i.e.,  $\alpha = 0$ ), and run the code to two relaxation times; we called the conditions at one and two relaxation times IC-I and IC-II, respectively.

To run the simulation, we turn on the cloud dispersion (i.e.,  $\alpha \neq 0$ ), after zero, one or two relaxation times accordingly.

Fig. 3 shows the  $xy$ -projection of the spatial and velocity distributions of different initial conditions. For IC-0, stars are restricted within 1 pc, and the velocity distribution has a very sharp upper limit. For IC-1 and IC-II, the cluster has smoother spatial and velocity distributions.

### 2.2.2 Stellar mass function

Goodwin (1997) mentioned that there is no significant difference between including a stellar mass function or not. However, for completeness and for comparison, we consider clusters with and without mass function. In both cases, the number of stars is 2500 and the total mass of the cluster is  $2500 M_\odot$ . In cluster with equal mass stars, each star is  $1 M_\odot$ . In cluster with a stellar mass function, we adopt Salpeter mass function with slope -2.35 (Salpeter (1955)) and mass range from 0.32 to  $32 M_\odot$ .

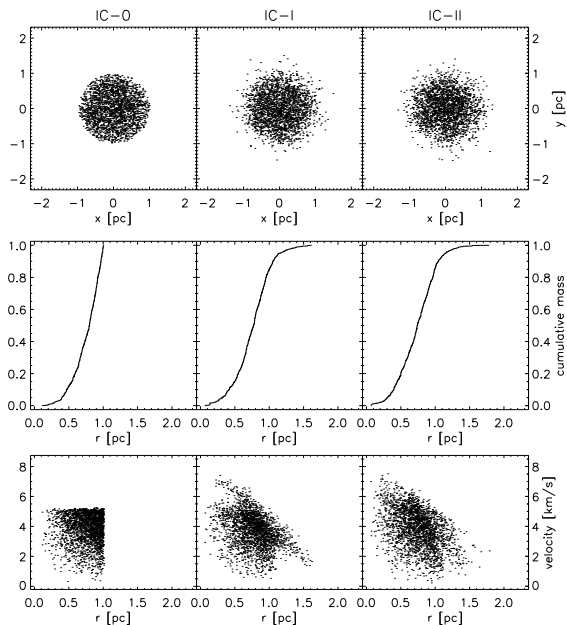


**Figure 3.**  $xy$ -projection of the spatial, mass and velocity distributions in radius of stars for the initial conditions IC-0, IC-I and IC-II, which correspond to preparing the cluster conditions at 0, 1 and 2 relaxation times, respectively (see text for details).

### 3 RESULTS

In order to investigate the problem as thoroughly as we can, for each dispersion rate  $\alpha$ , each initial condition and each mass function, we perform four hundred simulation runs on the parameter space  $(M_b, a_0)$  as listed in Tables 2 & 3. We worked out five dispersion rates (see Table 1), three initial conditions (see §2.2.1), and two mass functions equal mass and Salpeter mass function, see §2.2.2).

To illustrate the main results, we present four typical cases as listed in Table 4:

- B14s,  $M_b = 7.0M_c$ ,  $a_0 = 2.375$  pc (loose cloud);
- B07h,  $M_b = 3.5M_c$ ,  $a_0 = 1.0$  pc (intermediate cloud);
- B10g,  $M_b = 5.0M_c$ ,  $a_0 = 0.875$  pc (intermediate cloud);
- B18e,  $M_b = 9.0M_c$ ,  $a_0 = 0.625$  pc (massive and compact cloud).

All of these cases have  $\alpha = 0.2$  (i.e.,  $t_e = 1.5$  Myr), with initial condition IC-0 and Salpeter mass function.

Fig. 4 shows how the half mass radii,  $r_h$ , vary with time for these four cases. In B14s (dash-dotted line),  $r_h$  increases only a little bit. In B07h (dashed line),  $r_h$  increases more than 2 times and becomes stable after 10 Myr. B10g (dotted line) behaves similar to B07h, but the time to become stable is longer. Generally,  $r_h$  increases in the first 5 to 10 Myr and then shrinks back. Cluster is considered survived in these three cases (B14s has a compact core, and B07h and B10g are called loose). In B18e (solid line),  $r_h$  increases almost linearly. Cases such as B18e,  $r_h$  will never decrease again and cluster is considered destroyed. More quantitative criteria for compact core-, loose- and destroyed-clusters will be given below.

**Table 4.** Typical cases

Run	$t_e$ [Myr]	$M_b$ [ $M_c$ ]	$a_0$ [pc]
B14s	1.5	7	2.375
B07h	1.5	3.5	1
B18e	1.5	9	0.625
B10g	1.5	5	0.875

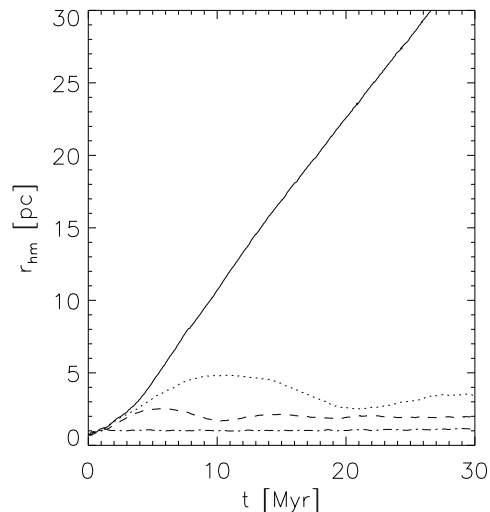


**Figure 4.** The evolution of half-mass radius  $r_h$ . Solid line is the destroyed case B18e. Dash-dotted line is the case with a compact core B14s. Dashed line and dotted line are loose cases B07h and B10g, respectively.

#### 3.1 Effect of cloud dispersion

The star cluster is in virial equilibrium in the potential well of the molecular cloud in the beginning. Every star is moving in a way according to how significant it is bound to the cloud and other stars. As the cloud is dispersing, its potential well is getting flatter and flatter, and its effect is negligible after 10 Myr. During this process, the cluster expands. Some stars may escape. If the expansion is not too serious, the cluster could adjust and return to equilibrium after some time, otherwise, it is on the way to destruction. From the velocity distribution, we can describe the evolution of the cluster in four stages as shown in Fig. 5. In the figure, the dots are stars, the solid lines are tracks of elliptical orbits which semi-major axes are 10, 15, 20, 25 and 30 pc.

- (1) bound: stars orbiting the centre of mass of the cluster at high speed because of the additional gravity provided by the cloud;
- (2) expansion: during (and after) cloud dispersion, stars seem to escape;
- (3) inner part formation: stars with shorter periods may pass their aphelion and return (following the solid lines which describe the Keplerian orbits);
- (4) final structure at 30 Myr: stars with longer periods may return, and return stars will forget their previous orbits due to the complex interaction in the inner part.

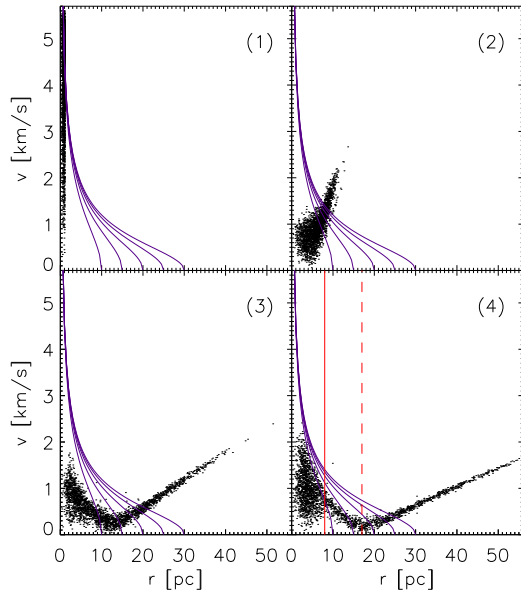


**Figure 5.** Different evolutionary stages of case E10i in  $\alpha=0.5$  ( $t_e=0.625$  Myr). Solid lines are tracks of elliptical orbit which semi-major axes are 10, 15, 20, 25 and 30 pc. There are four stages: (1) bound, (2) expansion, (3) inner part formation, and (4) final structure at 30 Myr. Red solid and dash lines in (4) separate inner part, return stars and stars do not reach their aphelion.

However, not every star could return if the dispersion of cloud is too serious. Our results show that the final structure can be grouped into three groups: (a) destroyed, (b) loose, and (c) compact core. Fig. 6 shows the three groups in the parameter space ( $M_b, a_0$ ). By examining the spatial distribution, we find that the boundaries can be well described by a parameter  $\epsilon$  which we called the expansion ratio. It is defined as the ratio between the final and initial  $r_{40}$  of the cluster,

$$\epsilon = \frac{r_{40,f}}{r_{40,i}}. \quad (6)$$

The boundaries are  $\epsilon \approx 2$  and 10. These numbers are chosen naively by examining the spatial distribution by eyes.

(a) destroyed ( $\epsilon > 10$ ): when clusters could not adjust themselves back to equilibrium in time, they will expand forever; e.g., case B18e;

(b) loose ( $10 > \epsilon > 2$ ): most clusters could adjust back to equilibrium but may become looser and loose part of stars; e.g., cases B07h and B10g;

(c) compact core ( $2 > \epsilon$ ): in some cases,  $r_{40}$  expands slightly (less than twice), they become stable and develop a denser, e.g. case B14s.

Fig. 7 shows the  $xy$ -projection of the final spatial distribution of the cluster of the cases B18E, B07h, B10g and B14s. Note that they have the same cloud dispersion rate.

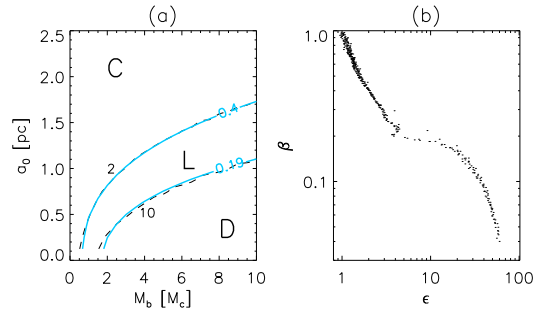


**Figure 6.** Groups in the cases with  $t_e=1.5$  Myr and Salpeter mass function. (a) Three generic groups: destroyed (D), loose (L), and compact core (C) are shown in the parameter space ( $M_b, a_0$ ). The dashed lines are the expansion ratio  $\epsilon = 2$  and 10. The solid lines are cluster-cloud mass ratio  $\beta = 0.40$  and 0.19, respectively. The two sets resemble each other very well (they almost overlap with each other). (b) Relation between  $\epsilon$  and  $\beta$ . Each points on the figure is a simulation run (there are 400 points). It appears linear for  $\epsilon < 5$ , there is a lack of data in the interval  $5 < \epsilon < 10$  and for  $\epsilon > 10$  some other relation takes over.

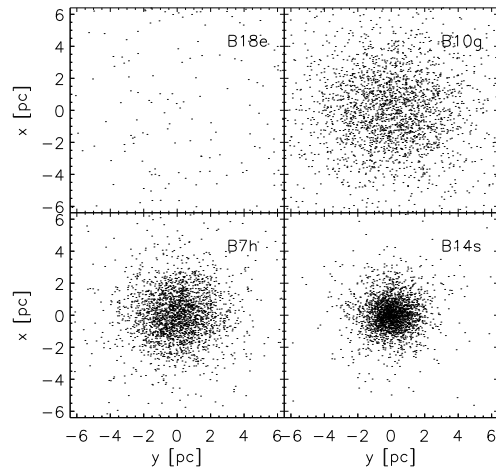


**Figure 7.**  $xy$ -projection of the spatial distribution of the cluster at 30 Myr. There are three generic types: destroyed (B18e), loose (B07h & B10g), compact core (B14s).

### 3.2 Cluster-cloud mass ratio and expansion ratio at $r_{40}$

As the cluster is bound by the parent cloud and its member stars initially. One would expect the more compact the cluster is the more the cluster will expand when the cloud is dispersed. After some experimentation, we find that the best parameters to delineate this anti-correlation is the initial cloud-cluster mass ratio  $\beta$  and the expansion ratio  $\epsilon$ , both define at the 40% Lagrangian radius of the cluster  $r_{40}$ . Fig. 6b shows how tight the correlation is. We should point out that if we define the cloud-cluster mass ratio and the expansion ratio with respect to other Lagrangian radii (say, 30% to 50%), we get qualitatively similar results but the correlation is not as good as the 40% Lagrangian radius. We

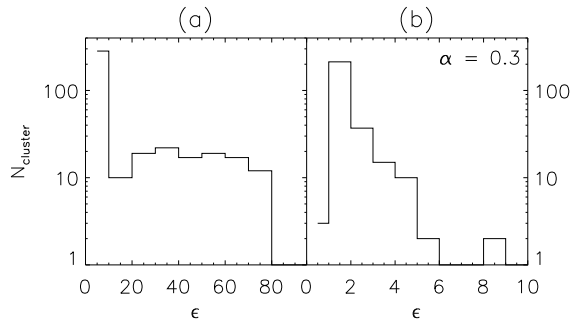


**Figure 8.** Histogram of  $\epsilon$  for  $t_e=1.1$  Myr. (a) Histogram from  $\epsilon=0$  to 100. About 300 cases (out of a total 400) are under 10. (b) Histogram from  $\epsilon=0$  to 10. Most are under 2 and the number drops off as  $\epsilon$  increases.

**Table 5.** The value of  $\beta$  corresponding to  $\epsilon = 2$  and 10.

$t_e$ [Myr]	3.3	1.5	1.1	0.75	0.625
$\beta_2$ ( $\beta$ at $\epsilon = 2$ )	0.40	0.40	0.40	0.45	0.50
$\beta_{10}$ ( $\beta$ at $\epsilon = 10$ )	0.13	0.19	0.22	0.22	0.30

still do not understand what is so special about  $r_{40}$  in our system.

It is worthwhile to mention the statistics of  $\epsilon$  in our simulation sample (with same dispersion rate and mass function). A typical result is shown in Fig. 8, which shows the histogram of the number of runs resulting in  $\epsilon$ . Clearly, most of the runs lie in  $\epsilon < 10$  and for  $\epsilon > 10$  the data seems to be evenly distributed (Fig. 8a). When we zoom into  $0 < \epsilon < 10$ , we find that there is a drop off in  $2 < \epsilon < 5$ , and within  $5 < \epsilon < 10$  there is almost no data (Fig. 8b). It seems that there is a transition region between 5 to 10.

### 3.3 Dispersion rates

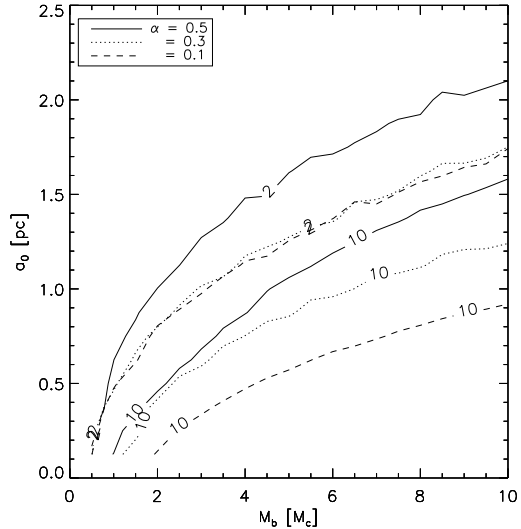
We work out five dispersion rates of the cloud with e-fold time  $t_e$  is from 0.625 to 3.3 Myr (see Table 1). Fig. 9 shows the  $r_{40}$  expanding ratio  $\epsilon$  of three dispersion rates (with e-fold time  $t_e = 3.3, 1.1, 0.625$  Myr) with the same initial condition (IC-0). The  $\epsilon \approx 2$  lines of the cases  $t_e = 3.3$  and 1.1 Myr almost overlap. As expected the region for destroyed cluster ( $\epsilon > 10$ ) is larger for  $t_e=0.625$  Myr (the most rapid dispersion rate in our simulations). In any case, many (more than two-third) of the clusters survive and remain intact 30 Myr after the cloud started to disperse.

Fig. 10 shows the relation between  $\epsilon$  and  $\beta$  for all five dispersion rates. Except  $t_e=0.625$  ( $\alpha=0.5$ ), all of them look alike when  $\epsilon < 5$  (dashed line is  $\epsilon = 5$ ). Even for  $t_e=0.625$ , the trend ( $\beta$  is larger when  $\epsilon$  is smaller) is the same as the others.

From Fig. 10 we can read the corresponding value of  $\beta$  for  $\epsilon = 2$  and 10 for the five dispersion rates. The result is listed in Table 5.

### 3.4 Initial conditions in virial equilibrium

Similar works usually start the cluster from virial equilibrium state. However cluster in virial equilibrium might not



**Figure 9.** The three generic groups in different dispersion rate (cf, Fig. 6a). Solid line is for  $\alpha=0.5$  ( $t_e=0.625$  Myr), dotted line is for  $\alpha=0.3$  ( $t_e=1.1$  Myr) and dashed line is for  $\alpha=0.1$  ( $t_e=3.3$  Myr). For  $\alpha=0.1$  and 0.3, the  $\epsilon \approx 2$  lines almost overlap, and although there is a separation in the  $\epsilon = 10$  lines, they just look like a shifting. For  $\alpha=0.5$ , the most rapid dispersion, although it looks a little different than the other two, we can still divide it to the three generic groups.

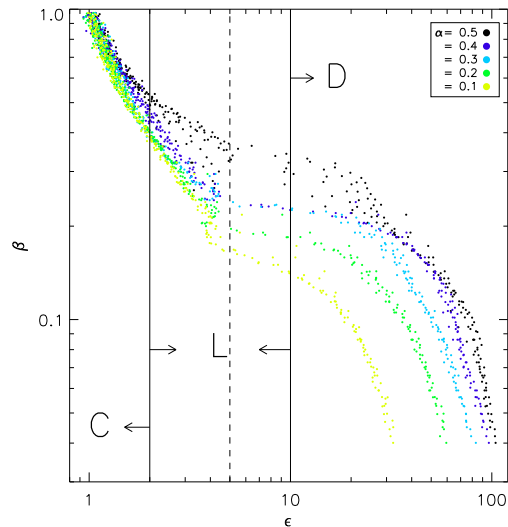


**Figure 10.** Relation between  $\epsilon$  and  $\beta$  for different dispersion rates. The relations are fairly similar for the cases  $\alpha = 0.1, 0.2, 0.3$  and 0.4. It is kind of different for  $\alpha = 0.5$ , but we can still use the solid lines  $\epsilon = 2$  and 10 to separate the destroyed, loose and compact core groups.

necessary in dynamical equilibrium (e.g, Goodwin (1997) and our tests, a brief description of our tests is given in §2.2.1). We would like to know whether this would make a difference. Thus we consider three different initial conditions according to the prescription mentioned in §2.2.1 (IC-0, IC-1, IC-2 for conditions taken at 0, 1, 2 relaxation times).

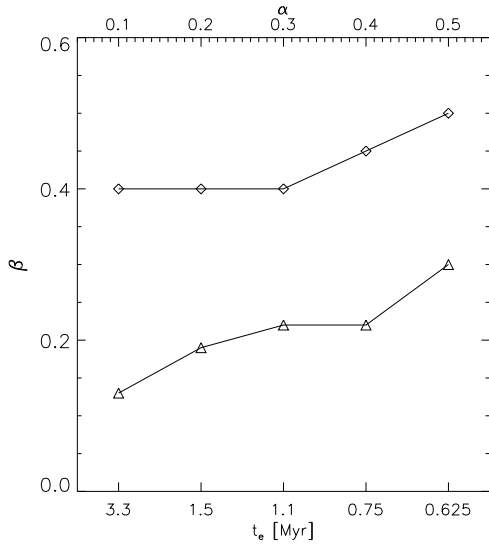


**Figure 11.** The relation between  $\alpha$  and  $\beta$  (or  $t_e$  and  $\beta$ ) for  $\epsilon = 2$  (diamond and the upper line) and 10 (triangle and the lower line).

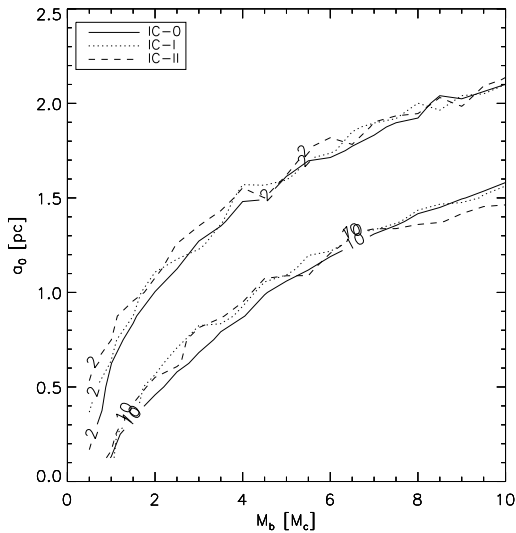


**Figure 12.** The three generic groups for  $t_e = 0.625$  Myr in different initial conditions. Solid line, dotted line and dashed line are for IC-0, IC-I and IC-II, respectively. There is no significant difference between these three models. Nonetheless IC-0 has the smoothest boundaries.

Fig. 12 shows the results of  $t_e = 0.625$  Myr for different initial conditions. The results agree with each other reasonably well. Nonetheless IC-0 gives the smoothest divisions. Similar results are seen in other models.

### 3.5 Stellar mass function and mass segregation

Previous works, such as Goodwin & Bastian (2006); Bastian & Goodwin (2006), claimed that simulations with equal mass and with mass function should give similar outcome. For completeness, we re-examine this issue. All the results presented so far are cases with Salpeter mass func-

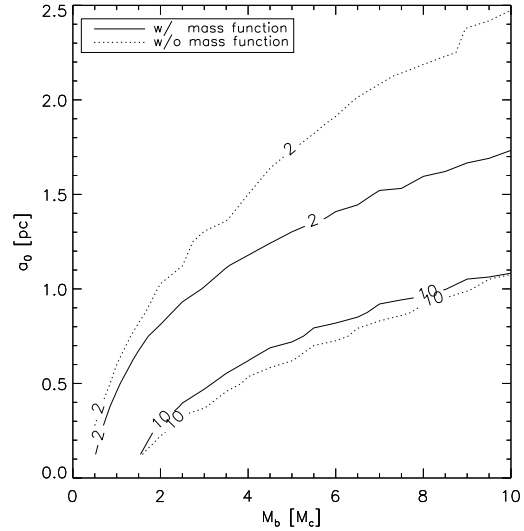


**Figure 13.** The three generic groups in different mass functions. The dispersion e-fold time of the cloud is  $t_e = 1.5$  Myr. Solid line is clusters with Salpeter mass function and dotted line is clusters with equal mass. The lines of  $\epsilon = 10$  agree well with each other, but the lines of  $\epsilon = 2$  are quite different, which is supposed to be a result of mass segregation.

tion (see §2.2.2). We repeat all the simulations for clusters with equal mass (i.e., each star is  $1 M_\odot$ ). Note that the number of stars and the total mass of the cluster are the same as those clusters with mass function (see §2.2.2).

The three generic groups: destroyed, loose and compact core are still applicable in the case of equal mass clusters. Fig. 13 compares the results with and without mass function in the same dispersion rate and the same initial condition (IC-0). In the figure, the solid lines are clusters with Salpeter mass function and the dotted lines are clusters with equal mass. While the boundaries separating the loose group and destroyed group for the two mass functions agree well with each other, the lines separating the loose group and compact core group do not. This is true for every dispersion rate. We conclude that only the boundary between loose group and destroyed group does not depend on mass function. The boundary between loose group and compact core group are different and may be attributed to mass segregation.

The concentration ratio for surviving clusters should be affected by mass function. Even for lower cluster-cloud mass ratio  $\beta$  could form a dense core in model with mass function. Examining mass distribution at later time, one should find that there is (and should be) mass segregation for cases with mass function. Fig. 14 shows the mass function of case C14s at 30 Myr (the end of our simulation). Since we do not have stellar evolution, there is no mass loss during the simulation. The mass function for the whole cluster remains Salpeter (solid line). In the inner region (1 pc, dashed line) the mass function is shallower, while in the outer region (between 1 to 1.5 pc, dotted line) the mass function is steeper or at least the region has less massive stars.

To learn how dispersion rates and initial conditions affect mass segregation, we plot the slope of the mass function against the cluster-cloud mass ratio  $\beta$  (Figs. 15 & 16). The general trend is the mass function is shallower when  $\beta$  is

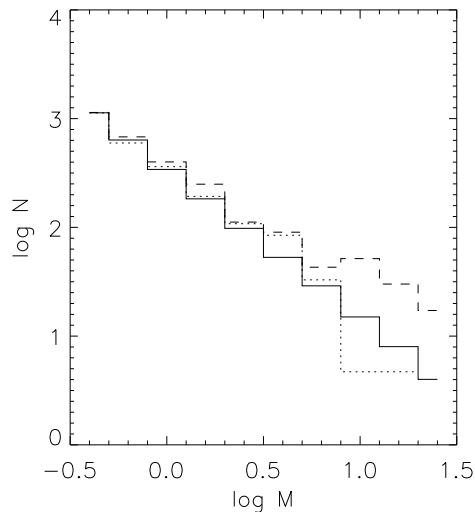


**Figure 14.** Mass segregation of case C14s at 30 Myr (the end of our simulation). Solid line, dashed line, dotted line are the mass functions for the whole cluster (Salpeter), for stars within 1 pc (shallower than Salpeter), for stars between 1 pc to 1.5 pc (steeper than Salpeter), respectively. Note that all the first bins are scaled to the same number.

smaller, i.e., mass segregation is more serious at smaller  $\beta$ . This can be understood as less massive stars are more likely to escape. (Recall that the cluster-cloud mass ratio  $\beta$  and the  $r_{40}$  expansion ratio  $\epsilon$  are anti-correlated, see Fig. 10 or 6b.)

In Fig. 15, there is little difference between different dispersion rates when  $\beta > 0.5$ . For smaller  $\beta$  (i.e., when cloud dominates over cluster in the beginning), the data scatter a lot. The reason might be the number of stars remains in the cluster is small in these cases, and the statistics is not very good.

In Fig. 16, besides more serious mass segregation at small  $\beta$ , there is another increase in mass segregation when  $\beta \geq 0.8$  for IC-I and IC-II. The reason can be traced back to the preparation of the initial conditions. For IC-I and IC-II, the cluster has already had some mass segregation in the beginning. It segregates more when  $\beta$  is large. After cloud dispersion, it becomes even more segregated.

### 3.6 Infant mortality

It is conceivable that the dispersion of a molecular cloud may destroy its embedded infant star clusters. The question is how effective is the process. From our simulation results, we deem that the process is not very effective. Infant clusters can be destroyed only when the  $r_{40}$  cluster-cloud mass ratio  $\beta$  is below some value. Specifically,  $\beta < \beta_{10}$  ( $\beta$  at  $\epsilon = 10$ ) in Table 5 (also see Fig. 11). From the cases we considered, many infant clusters survive (some of them are loosened while some develop a compact core). Table 6 presents the frequency of the three groups (destroyed, loose, compact core) for different cloud dispersion rates and mass functions. Roughly 20% to 40% (e-fold time from 3.3 Myr to 0.625 Myr) will be destroyed. More than 30% for equal

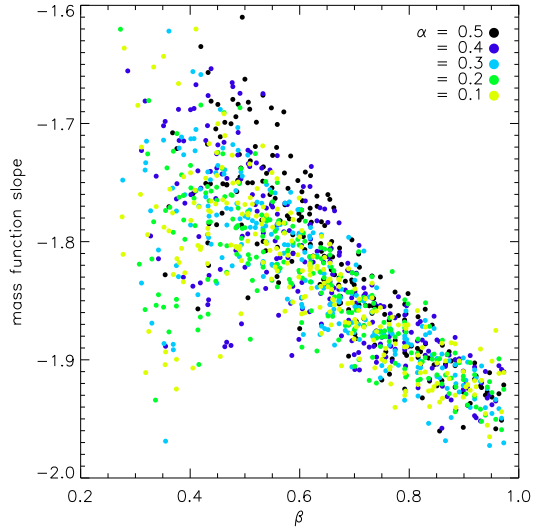


**Figure 15.** Slope of mass function (within initial  $r_h$ ) against cluster-cloud mass ratio for different dispersion rates. The mass function of initial condition is Salpeter with slope -2.35. The general trend is more serious mass segregation when  $\beta$  is smaller. The scattering in small  $\beta$  might be due to the number of stars is small at 30 Myr (the end of simulation).

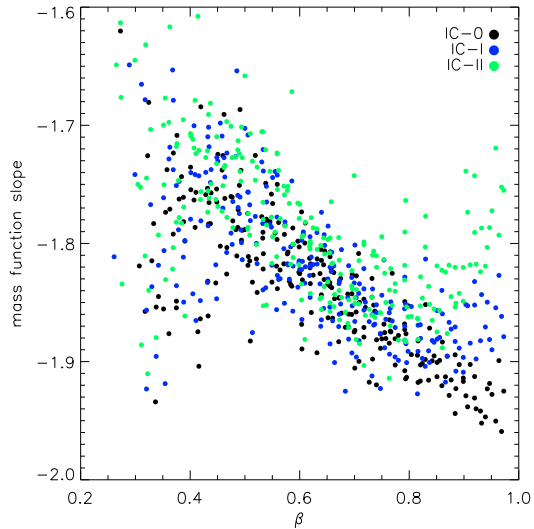


**Figure 16.** Slope of mass function (within initial  $r_h$ ) against cluster-cloud mass ratio for the three initial conditions (§2.2.1). The cloud dispersion e-fold time is  $t_e = 1.5$ . The general trend is more serious mass segregation when  $\beta$  is smaller. However, when  $\beta \geq 0.8$  there is another increase in mass segregation for IC-I and IC-II (see text for a possible explanation).

mass clusters and more than 40% for Salpeter mass function develop a compact core.

We should point out that the boundaries ( $\epsilon = 2$  and 10) between the three groups compact core, loose and destroyed are determined partly by eyes (from the spatial, velocity and mass distribution such as in Fig. 7) and partly by numbers (such as the histograms in Fig. 8). The boundaries between

**Table 6.** Infant mortality in %

Salpeter					
$t_e$ [Myr]	3.3	1.5	1.1	0.75	0.625
Compact core	55	54	54	49.25	42.75
Loose	26	22	16.75	21.75	21
Destroyed	19	24	29.25	29	36.25
equal mass					
$t_e$ [Myr]	3.3	1.5	1.1	0.75	0.625
Compact core	37.5	36.5	35.5	32.5	30
Loose	45	42.25	38.5	38	37.75
Destroyed	17.5	21.25	26	29.5	32.25

loose and destroyed ( $\epsilon = 10$ ) we pick may not be precise. However, we claim that the exact location of the boundary (if there is an extra one) does not affect the estimated destroyed frequency listed in Table 6. As we discussed in §3.2 there is a transition zone between  $\epsilon = 5$  to 10 where only very few cases exist (see Fig. 8). As the boundary is somewhere around  $\epsilon \approx 10$  (within the transition zone), the exact location will not matter too much on the estimated frequency for the two classes (destroyed and loose).

We should point out that the range of the transition region is actually slightly different for different dispersion rates (see Fig. 10). In most cases, the transition region runs from  $\epsilon = 5$  to 15 (for slow dispersion, such as  $t_e = 3.3$  Myr) and 5 to 30 (for rapid dispersion, such as  $t_e = 0.625$  Myr). The exact location does not matter too much on the results as there are only very few cases inside the transition region.

#### 4 SUMMARY AND REMARKS

Can a bound star cluster in a molecular cloud survive when the parent cloud is dispersed? We studied this problem by means of N-body simulations. The dispersion of the cloud makes the cluster to expand or even dissociate as the binding energy decreases. However, our simulations show that this process is ineffective in destroying the bound cluster.

The dispersion of the cloud is modelled by a Plummer potential with expanding length scale. We numerically simulated the behaviour of a bound cluster in this potential up to 30 Myr. We performed numerous simulations and concluded that there are three groups of final morphology: compact core, loose and destroyed. It turns out that the 40% Lagrangian radius expansion ratio of the cluster  $\epsilon$  (the ratio of  $r_{40}$  at 30 Myr to initial, see Eq. (6)) is a good indicator for the final fate of the cluster. More importantly, we found that the initial  $r_{40}$  cluster-cloud mass ratio  $\beta$  (see Eq. (4)) is tightly correlated with  $\epsilon$ . Hence we can “predict” the fate of the embedded bound cluster by examining its  $\beta$ .

The survival probabilities are high when  $\beta$  is high. After 30 Myr, more than 70% of the clusters still remain a shape of clusters, with a number density higher than  $15/\text{pc}^3$  within 1 pc radius. Different cloud dispersion rates provide similar results and even the largest rate in our simulations (e-fold time  $t_e = 0.625$  Myr) does not disrupt all the clusters. Systems with and without mass function have different final densities but agree with each other well.

We conclude that the infant mortality rate should be low if the embedded clusters are bound from the beginning, unless  $\beta$  is less than about 0.13 (for slow dispersion, such as  $t_e = 3.3$  Myr) to 0.30 (for rapid dispersion, such as  $t_e = 0.625$  Myr) (see Table 5).

Near infrared observations indicate that the survival probability for embedded clusters is about 4% to 7% (Lada & Lada (2003)). How should we reconcile our result with the observations? We deem that the dispersion of parent cloud can not account for the destruction of embedded bound clusters. Therefore, other more effective mechanisms must be responsible or the stars formed in molecular cloud are not bound (see e.g., Bonnell et al. (2006)).

#### ACKNOWLEDGMENTS

We appreciate Alessia Gualandris for her kindly and very helpful discussions. This work was supported in part by the National Science Council, Taiwan under the grants NSC-95-2112-M-008-006 and NSC-96-2112-M-008-014-MY3.

#### REFERENCES

- Aarseth, S.J. 2001, *New Astronomy*, 6, 277  
Baumgardt, H. & Kroupa, P. 2007, *MNRAS*, 380, 1589  
Bastian, N. & Goodwin, S.P. 2006, *MNRAS*, 369, L9  
Blitz, L. & Shu, F. 1980, *ApJ*, 238, 148  
Boily, C.M. & Kroupa, P. 2003a, *MNRAS*, 338, 665  
Boily, C.M. & Kroupa, P. 2003b, *MNRAS*, 338, 673  
Bonnell, I. A., Dobbs, C. L., Robitaille, T. P., Pringle, J.E. 2006, *MNRAS*, 365, 37  
Chandar, R., Fall, S. M., Whitmore, B. C. 2006, *ApJ*, 650, L111  
Elmegreen, B. 2000, *ApJ*, 530, 277  
Fall, S. M., Chandar, R., Whitmore, B. C. 2005, *ApJ*, 631, L133  
Gieles, M., Portegies Zwart, S.F., Baumgardt, H., Athanassoula, E., Lamers, H.J.G.L.M., Sipior, M. & Leenaarts, J. 2006, *MNRAS*, 371, 793  
Hartmann, L., Balestros-Paredes, J., Bergin, E. A. 2001, *ApJ*, 562, 852  
Goodwin, S.P. 1997, *MNRAS*, 284, 785  
Goodwin, S.P. & Bastian, N. 2006, *MNRAS*, 373, 752  
Lada, C.J. & Lada, E.A. 2003, *ARA&A*, 41, 57  
Lada, C.J., Margulis, M., Dearborn, D. 1984, *ApJ*, 285, 141  
Leisawitz, D., Bash, F. N., Thaddeus, P. 1989, *ApJS*, 70, 731  
Pellerin, A., Meyer, M., Harris, J., Calzetti, D. 2007, *ApJL*, 658, 87  
Salpeter, E.E. 1955, *ApJ*, 121, 161  
Williams, J. & McKee, C.F. 1997, *ApJ*, 476, 166